Published for SISSA by Springer

Received: *August 20, 2023*
Revised: *November 3, 2023*
Accepted: *November 18, 2023*
Published: *December 1, 2023*

Flavour constraints on light spin-1 bosons within a chiral Lagrangian approach

Luca Di Luzio,[a] **Gabriele Levati,**[a,b] **Paride Paradisi**[a,b] **and Xavier Ponce Díaz**[a,b]

[a]*Istituto Nazionale di Fisica Nucleare (INFN), Sezione di Padova, Via F. Marzolo 8, 35131 Padova, Italy*
[b]*Dipartimento di Fisica e Astronomia 'G. Galilei', Università di Padova, Via F. Marzolo 8, 35131 Padova, Italy*

E-mail: luca.diluzio@pd.infn.it, gabriele.levati@pd.infn.it, paride.paradisi@pd.infn.it, xavier.poncediaz@pd.infn.it

Abstract: We discuss the construction of the chiral Lagrangian for a light spin-1 boson, here denoted as X, featuring both vector and axial-vector couplings to light u, d, s quarks. Focusing on $\Delta S = 1$ transitions, we show that there are model-independent tree-level contributions to $K^\pm \to \pi^\pm X$, sourced by Standard Model charged currents, which receive an m_K^2/m_X^2 enhancement from the emission of a longitudinally polarized X. This flavour observable sets the strongest to date model-independent bound on the diagonal axial-vector couplings of X to u, d, s quarks for $m_X < m_K - m_\pi$, superseding the bounds arising from beam-dump and collider searches.

Keywords: Chiral Lagrangian, New Light Particles, Rare Decays, New Gauge Interactions

ArXiv ePrint: 2308.05215

https://doi.org/10.1007/JHEP12(2023)016

Contents

1 Introduction

The lack of new particles at the LHC may be suggestive of the fact that they are either too heavy to be directly produced or too weakly coupled to Standard Model (SM) particles. New Physics (NP) models containing new feebly interacting massive particles with sub-GeV masses are currently among the most studied NP scenarios both theoretically and experimentally. Many of these studies were dedicated to the dark photon [1, 2], a new massive spin-1 particle which is kinetically mixed with the ordinary photon and that could act as a portal to a dark sector. Dark photon searches have been conducted by a number of experiments, including beam-dump [3], fixed-target [4, 5], collider [6–12], as well as meson decay [13–19] experiments.

Moreover, comprehensive analyses aiming at probing a light spin-1 boson X with general couplings to quarks and leptons have been also carried out (see e.g. [20–23]). If X is coupled to SM particles through a non-conserved current, such as the axial-vector current, processes which are enhanced by the ratio $(\text{energy}/m_X)^2$ of X are generally induced.[1] The same happens if X is coupled to a tree-level conserved current which is broken by the chiral anomaly [28, 29]. These energy-enhanced contributions generally provide the dominant effects both to the production mechanisms of X in high-energy experiments, as well as to flavor-changing neutral current processes such as $K^\pm \to \pi^\pm X$.

The aim of this paper is to revisit the sensitivity to the above NP scenarios of the rare decay $K^\pm \to \pi^\pm X$ induced by an underlying $s \to d$ quark transition. In order to accomplish

[1]This effect was first noticed in ref. [24], and several experimental directions were proposed in order to exploit such an enhancement, including parity-violating effects [25], meson resonances decays [26] and flavour-violating processes [27].

JHEP12(2023)016

this task, we will extend previous studies by constructing the most general $\Delta S = 1$ chiral Lagrangian up to the order $\mathcal{O}(p^4)$, which will enable us to account for all of the dominant effects stemming from weak interactions. Indeed, the lowest-order $\mathcal{O}(p^2)$ terms of chiral perturbation theory (χPT) will capture the weak effects to the $s \to dX$ transition discussed in [28, 29] and arising from the one-loop exchange of the W-boson and up-quarks. Instead, as we will see, weak effects stemming from the $\Delta S = 1$ four-quark Lagrangian [30], can be included only by keeping $\mathcal{O}(p^4)$ terms in χPT. Although subleading in the chiral expansion, the latter contributions to $K^\pm \to \pi^\pm X$ arise already at tree level (they can be thought as arising from initial or final state radiation of X from the external quark legs of the $\Delta S = 1$ effective Lagrangian) and therefore their inclusion appears to be mandatory.

Moreover, the tree-level weak contributions discussed in this work are model-independent and therefore they represent a general and robust prediction of any ultraviolet (UV) complete NP model entailing a light spin-1 boson. Instead, the loop-induced effects discussed in [28, 29] are sensitive to the specific UV completion responsible for the mass generation of X (see e.g. [31]).

The paper is organised as follows. In Section 2, we will present the general derivation of the $\Delta S = 1$ chiral Lagrangian, as well as the related Feynman rules for spin-1 bosons up to the $\mathcal{O}(p^4)$ order. In Section 3, we will compute the $K^\pm \to \pi^\pm X$ decay rate in χPT exploiting the Feynman rules derived in Section 2, comparing our tree-level effects with the results obtained at one-loop level in [28, 29]. In Section 4, we will discuss our flavour bounds vs. beam-dump and collider searches as reported in [21, 22]. Section 5 is dedicated to our conclusions, while more technical details about the construction of the chiral Lagrangian are deferred to appendix A.

2 $\Delta S = 1$ chiral Lagrangian for spin-1 bosons

The most general Lagrangian describing the lowest-order interactions of a new spin-1 particle X with SM fermions includes both vectorial and axial couplings and, focusing on the interactions with the lightest quark flavours $q = (u, d, s)^T$, it can be written as

$$\mathcal{L}_X^{\text{int}} = g_x X_\mu \bar{q} \gamma^\mu (x_V + x_A \gamma_5) q \,, \tag{2.1}$$

where g_x measures the strength of the universal coupling of X to quarks. The vectorial and axial charges, $x_{V,A}$, are defined in flavour space and include off-diagonal entries in the 2-3 sector.

2.1 Lowest-order chiral Lagrangian

At energies above few GeV, the Lagrangian of eq. (2.1) can be directly employed to analyse the interactions of X_μ with quarks. Here, instead we focus on the low-energy range below the GeV scale, where we can resort to χPT — see e.g. [32, 33]. In order to construct our χPT in the presence of X_μ, we proceed as follows. Let us consider the massless QCD Lagrangian with chiral symmetry group $G = \text{SU}(3)_L \times \text{SU}(3)_R$

$$\mathcal{L}^0_{\text{QCD}} = -\frac{1}{4} G^a_{\mu\nu} G_a^{\mu\nu} + i\bar{q}_L \gamma^\mu \left(\partial_\mu + i g_s \frac{\lambda_a}{2} A^a_\mu \right) q_L + i\bar{q}_R \gamma^\mu \left(\partial_\mu + i g_s \frac{\lambda_a}{2} A^a_\mu \right) q_R \,, \tag{2.2}$$

where $q = (u, d, s)^T$ and λ_a are the Gell-Mann matrices.

Chiral symmetry-breaking terms (like mass terms or interactions with external gauge fields other than gluons) can be implemented by introducing appropriate spurions (a_μ, v_μ, s, p) as external source fields [32]. Therefore, the resulting Lagrangian $\mathcal{L}_{\rm QCD}^{\rm ext}$ reads

$$\begin{aligned}\mathcal{L}_{\rm QCD}^{\rm ext} &= \mathcal{L}_{\rm QCD}^{0} + \bar{q}\gamma^\mu(v_\mu + a_\mu\gamma_5)q + \bar{q}(s - ip\gamma_5)q \\ &= \mathcal{L}_{\rm QCD}^{0} + \bar{q}\gamma^\mu(2r_\mu P_R + 2\ell_\mu P_L)q + \bar{q}(s - ip\gamma_5)q\,.\end{aligned} \tag{2.3}$$

where $2r_\mu = v_\mu + a_\mu$ and $2\ell_\mu = v_\mu - a_\mu$. Its chiral counterpart is then found to be

$$\mathcal{L}_{\chi\rm PT}^{\rm ext} = \frac{f_\pi^2}{4}{\rm Tr}\left[D_\mu U^\dagger D^\mu U + U^\dagger\chi + \chi^\dagger U\right] + \mathcal{O}(p^4) \tag{2.4}$$

where ${\rm U}(x) = \exp\left[i\lambda_a\pi_a(x)/f_\pi\right]$ (with $f_\pi \simeq 92\,{\rm MeV}$) is the mesonic matrix transforming as ${\rm U}(x) \to L{\rm U}(x)R^\dagger$ under ${\rm SU(3)}_L \times {\rm SU(3)}_R$ and $\pi_a(x)$ are the Goldstone boson fields of ${\rm SU(3)}_L \times {\rm SU(3)}_R \to {\rm SU(3)}_V$ spontaneous breaking. Moreover, we have defined

$$D_\mu U = \partial_\mu U - ir_\mu U + iU\ell_\mu \qquad \text{and} \qquad \chi = 2B_0\,(s + ip)\,. \tag{2.5}$$

In our model, described by the Lagrangian of eq. (2.1), the covariant derivative $D_\mu U$ reads

$$D_\mu U = \partial_\mu U - ig_x X_\mu(Q_R^x U - UQ_L^x)\,, \tag{2.6}$$

where $Q_{R/L}^x = Q_V^x \pm Q_A^x$, while

$$Q_V^x = \begin{bmatrix} x_V^u & 0 & 0 \\ 0 & x_V^d & x_V^{23} \\ 0 & x_V^{32} & x_V^s \end{bmatrix} \qquad \text{and} \qquad Q_A^x = \begin{bmatrix} x_A^u & 0 & 0 \\ 0 & x_A^d & x_A^{23} \\ 0 & x_A^{32} & x_A^s \end{bmatrix} \tag{2.7}$$

Expanding the Lagrangian in (2.4) and keeping only the lowest order terms in the NP coupling, we find

$$\begin{aligned}\mathcal{L}_{\chi\rm PT}^{\rm ext} \supset & -ig_x X_\mu(x_V^u - x_V^s)\left(\partial^\mu K^- K^+ - \partial^\mu K^+ K^-\right) - iX_\mu g_x(x_V^u - x_V^d)\left(\partial^\mu\pi^-\pi^+ - \partial^\mu\pi^+\pi^-\right) \\ & + \left[-ig_x X_\mu x_V^{32}\left(\partial^\mu K^+\pi^- - \partial^\mu\pi^- K^+\right) + {\rm h.c.}\right],\end{aligned} \tag{2.8}$$

with the corresponding Feynman rules given in figure 1 (all momenta flow from left to right).

Note that all couplings in eq. (2.8) are of vector type. This is due to the fact that the matrix element of the axial-vector quark operators in eq. (2.1) vanishes between external pseudo-scalar meson states. Moreover, in the limit of universal vector couplings, i.e. $x_V^u = x_V^d = x_V^s$, the K^+K^-X and $\pi^+\pi^-X$ interaction terms vanish as well, as a result of the underlying ${\rm SU(3)}_V$ chiral symmetry, while the $K^+\pi^-X$ vector coupling still survives as the flavour-changing current is not conserved.

Moreover, tree-level contributions to $\Delta S = 1$ processes, such as $K^\pm \to \pi^\pm X$, are generated only if the couplings x_V are flavor off-diagonal. Yet, even for flavour-diagonal couplings, irreducible flavour-violating effects to x_V are loop-induced by the exchange of the W boson and up-quarks (see e.g. [29]). In the following, we will show that weak interactions provide additional sources of flavour-violation to the $\Delta S = 1$ chiral Lagrangian, already at tree level, when we include higher-order terms in the momentum expansion corresponding to four-quark operators.

JHEP12(2023)016

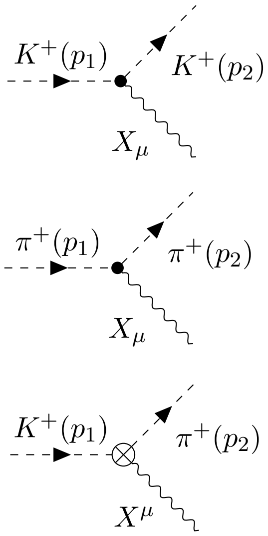

$$= ig_x(p_1+p_2)_\mu(x_V^u - x_V^s)$$

$$= ig_x(p_1+p_2)_\mu(x_V^u - x_V^d)$$

$$= -ig_x x_V^{32}(p_1^\mu + p_2^\mu)$$

Figure 1. Feynman rules for the lowest-order chiral Lagrangian.

2.2 Chiral Lagrangian for weak interactions

In the SM, at energies above the scale of chiral symmetry breaking, $\Delta S = 1$ transitions are induced by the effective four-fermion Lagrangian [30]

$$\mathcal{L}_{\rm SM}^{\Delta S=1} = G \sum_{i=1}^{10} C_i(\mu) O_i(\mu) \qquad \text{with} \qquad G \equiv -\frac{G_F}{\sqrt{2}} V_{ud} V_{us}^*\,, \tag{2.9}$$

where

$$\begin{aligned}
&Q_1 = 4(\bar{s}_L\gamma_\mu d_L)(\bar{u}_L\gamma_\mu u_L), && Q_2 = 4(\bar{s}_L\gamma_\mu u_L)(\bar{u}_L\gamma_\mu d_L),\\
&Q_3 = 4(\bar{s}_L\gamma_\mu d_L)(\bar{q}_L\gamma_\mu q_L), && Q_4 = 4(\bar{s}_L^\alpha\gamma_\mu d_L^\beta)(\bar{q}_L^\beta\gamma_\mu q_L^\alpha),\\
&Q_5 = 4(\bar{s}_L\gamma_\mu d_L)\textstyle\sum_q(\bar{q}_R\gamma_\mu q_R), && Q_6 = 4(\bar{s}_L^\alpha\gamma_\mu d_L^\beta)\textstyle\sum_q(\bar{q}_R^\beta\gamma_\mu q_R^\alpha),\\
&Q_7 = 6(\bar{s}_L\gamma_\mu d_L)\textstyle\sum_q e_q(\bar{q}_R\gamma_\mu q_R), && Q_8 = 6(\bar{s}_L^\alpha\gamma_\mu d_L^\beta)\textstyle\sum_q e_q(\bar{q}_R^\beta\gamma_\mu q_R^\alpha),\\
&Q_9 = 6(\bar{s}_L\gamma_\mu d_L)\textstyle\sum_q e_q(\bar{q}_L\gamma_\mu q_L), && Q_{10} = 6(\bar{s}_L^\alpha\gamma_\mu d_L^\beta)\textstyle\sum_q e_q(\bar{q}_L^\beta\gamma_\mu q_L^\alpha),
\end{aligned} \tag{2.10}$$

$q = u, d, s$, $e_u = 2/3$ and $e_d = e_s = -1/3$; α and β are colour indices which, if unspecified, are assumed to be contracted between the two quarks in the same current.

The construction of the chiral counterpart to eq. (2.10) proceeds in two steps:

- In the first step, one constructs the chiral structures describing the product of two fermionic currents. These structures must possess the same chiral transformation properties of the corresponding quark currents and are obtained by exploiting the quark-hadron duality between the Lagrangians of eqs. (2.3) and (2.4). At low energies, one has

$$\int \mathcal{D}q\,\mathcal{D}\bar{q}\,\mathcal{D}G_\mu \,\exp\left(i\int d^4x\,\mathcal{L}_{\rm QCD}^{\rm ext}\right) = \int \mathcal{D}U \exp\left(i\int d^4x\,\mathcal{L}_{\chi\rm PT}^{\rm ext}\right)\,, \tag{2.11}$$

JHEP12(2023)016

and taking the functional derivatives of the QCD and the χPT actions with respect to the external sources one can readily find the chiral counterparts to the various Dirac structures. For instance, up to order $\mathcal{O}(p^2)$ one finds

$$\begin{aligned}
\bar{q}^i_L\gamma^\mu q^j_L &= \frac{\delta S_{\rm QCD}}{\delta(\ell_\mu)_{ij}} \equiv \frac{\delta S_{\chi\rm PT}}{\delta(\ell_\mu)_{ij}} = \frac{i}{2}f_\pi^2(D^\mu U^\dagger U)_{ji} = -\frac{1}{2}f_\pi^2(L^\mu)_{ji}\,,\\
\bar{q}^i_R\gamma^\mu q^j_R &= \frac{\delta S_{\rm QCD}}{\delta(r_\mu)_{ij}} \equiv \frac{\delta S_{\chi\rm PT}}{\delta(r_\mu)_{ij}} = \frac{i}{2}f_\pi^2(D^\mu U U^\dagger)_{ji} = -\frac{1}{2}f_\pi^2(R^\mu)_{ji}\,,\\
\bar{q}^i_L q^j_R &= -\frac{\delta S_{\rm QCD}}{\delta(s-ip)_{ij}} \equiv -\frac{\delta S_{\chi\rm PT}}{\delta(s-ip)_{ij}} = -\frac{B_0}{2}f_\pi^2 U_{ji}\,,\\
\bar{q}^i_R q^j_L &= -\frac{\delta S_{\rm QCD}}{\delta(s+ip)_{ij}} \equiv -\frac{\delta S_{\chi\rm PT}}{\delta(s+ip)_{ij}} = -\frac{B_0}{2}f_\pi^2 (U^\dagger)_{ji}\,,
\end{aligned} \tag{2.12}$$

where in the previous expressions we have defined the chiral currents L_μ and R_μ

$$L_\mu \equiv iU^\dagger D_\mu U = -iD_\mu U^\dagger U\,, \qquad R_\mu \equiv iUD_\mu U^\dagger = -iD_\mu U U^\dagger\,. \tag{2.13}$$

- In the second step, one decomposes the product of quark currents into irreducible representations of the flavour algebra by defining appropriate projectors. These are to be applied as well to the chiral realisation of the quark currents in order to obtain the desired operators in the chiral Lagrangian, classified according to the irreducible representation of the flavour algebra they belong to (see e.g. [34–36]). Further details are discussed in appendix A.

After carrying out the program outlined above, we finally reproduce the $\Delta S = 1$ chiral Lagrangian of ref. [34], which takes the following simple form

$$\begin{aligned}
\mathcal{L}_{\rm eff}^{\Delta S=1} = G f_\pi^4 \Big\{ & g_{27}\left(L^3_{\mu,2}L^{\mu,1}_1 + \frac{2}{3}L^1_{\mu,2}L^{\mu,3}_1 - \frac{1}{3}L^3_{\mu,2}{\rm Tr}\,[L^\mu]\right) + g_8^S\, L^3_{\mu,2}{\rm Tr}\,[L^\mu]\\
&+ g_8\left({\rm Tr}\,[\lambda L_\mu L^\mu] + e^2 g_{\rm ew} f_\pi^2 {\rm Tr}\,\left[\lambda U^\dagger Q U\right]\right)\Big\}\,,
\end{aligned} \tag{2.14}$$

where $\lambda \equiv \frac{1}{2}(\lambda_6 - i\lambda_7)$ is responsible for the $s \to d$ flavour transition and we have specialised $Q = \frac{1}{3}{\rm diag}(2,-1,-1)$ to be the charge matrix for quarks. Out of the pieces making up eq. (2.14), the first one transforms in the $(27_L, 1_R)$ representation of the flavour group, while the second and the third ones transform in the $(8_L, 1_R)$ and $(8_L, 8_R)$ representation, respectively. Clearly, no singlet term can have any effect on $\Delta S = 1$ transitions. The coefficients g_{27}, g_8, g_8^S and $g_{\rm ew}$ are functions of non-perturbative effective parameters, as well as of the Wilson coefficients of the weak operators, see eq. (2.9). Their values are found to be

$$g_8 = 3.07 \pm 0.14 \qquad [34]\,, \tag{2.15}$$

$$g_8^S = -1.17 \pm 0.37 \qquad [37]\,, \tag{2.16}$$

$$g_{27} = 0.29 \pm 0.02 \qquad [34]\,, \tag{2.17}$$

$$g_{\rm ew} = -1.0 \pm 0.3 \qquad [38]\,. \tag{2.18}$$

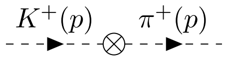

$$= i2f^2G\left[g_8(f^2e^2g_{\rm ew}+p^2)+\tfrac{2}{3}g_{27}p^2\right]$$

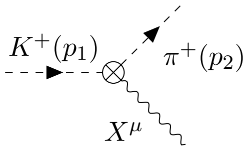

$$\begin{aligned}
&= ig_x 2f^2G\Big[g_8(p_1^\mu(x_A^u+x_A^s+x_V^u-x_V^d)+p_2^\mu(x_A^u+x_A^d+x_V^u-x_V^s))\\
&\quad +g_8^S(p_1^\mu+p_2^\mu)(x_A^u+x_A^d+x_A^s)+\tfrac{g_{27}}{3}(p_1^\mu(4x_A^u-3x_A^d-x_A^s+2x_V^u\\
&\quad -2x_V^d)+p_2^\mu(4x_A^u-x_A^d-3x_A^s+2x_V^u-2x_V^s))\Big]
\end{aligned}$$

Figure 2. Feynman rules for the chiral Lagrangian of weak interactions.

Expanding the Lagrangian of eq. (2.14) and keeping only the contributions relevant for our analysis, we find

$$\begin{aligned}
\mathcal{L}_{\rm eff}^{\Delta S=1} \supset\ & \frac{2}{3}f^2g_{27}G\Big(2\partial^\mu K^+\partial_\mu\pi^- + g_xX_\mu\Big[i\partial^\mu K^+\pi^-(4x_A^u-x_A^d-3x_A^s+2x_V^u-2x_V^d)\\
&-i\partial^\mu\pi^-K^+(4x_A^u-3x_A^d-x_A^s+2x_V^u-2x_V^d)+\text{h.c.}\Big]\Big)\\
&+2f^2g_8^SGg_x\left(x_A^u+x_A^d+x_A^s\right)X_\mu\Big[i\left(\partial^\mu K^+\pi^- - \partial^\mu\pi^-K^+\right)+\text{h.c.}\Big]\\
&+2f^2g_8G\Big(\partial^\mu K^+\partial_\mu\pi^- + g_xX_\mu\Big[i\partial^\mu K^+\pi^-(x_A^u+x_A^s+x_V^u-x_V^d)\\
&-i\partial^\mu\pi^-K^+(x_A^u+x_A^d+x_V^u-x_V^s)+\text{h.c.}\Big]\Big)+2f^4Ge^2g_8g_{\rm ew}K^+\pi^-\,,
\end{aligned} \tag{2.19}$$

which includes both a $K\pi$ mixing term as well as a flavour-violating $K^\pm\to\pi^\pm X$ interaction, as depicted in the Feynman rules of figure 2.

Note that, if eq. (2.1) contains an explicit source of flavour violation, the latter Feynman rule has to be supplemented by the last contribution displayed in figure 1.

Differently from the leading-order chiral Lagrangian of eq. (2.8), we are now sensitive both to x_V^f and x_A^f couplings. Indeed, the hadronic matrix element $\langle K|O_i|\pi\rangle$, where O_i are the weak operators defined in eq. (2.10), receives contributions from both vector and axial-vector currents, as there are not symmetry arguments to forbid them. Again, for universal vector couplings, the $K^+\pi^-X$ interaction vanishes because of the underlying $\mathrm{SU}(3)_V$ chiral symmetry.

3 $K^\pm\to\pi^\pm X$ in χPT

In this section we will compute the decay rate of the process $K^\pm\to\pi^\pm X$ in χPT. Exploiting the Feynman rules derived in the previous section, we will first analyse the tree-level contributions and then we will compare them with the results obtained at one-loop level in [28].

3.1 Tree-level contribution

At the tree level, the process $K^\pm\to\pi^\pm X$ is generated by the diagrams in figure 3. The X boson can be emitted either at the same vertex where the flavour transition takes place (first diagram) or at a different one. In the latter case (second and third diagrams) weak

JHEP12(2023)016

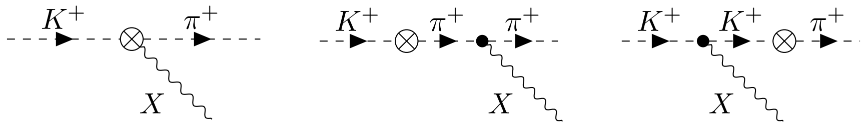

Figure 3. Diagrams generating the tree-level transition $K^\pm \to \pi^\pm X$ in χPT.

interactions prompt a flavour transition while the leg emission of an X boson occurs at a different interaction point.

The total amplitude $\mathcal{M} = \mathcal{M}_8 + \mathcal{M}_8^S + \mathcal{M}_{27} + \mathcal{M}_{\rm ew}$ receives four independent contributions proportional to g_8, g_8^S, g_{27} and $g_{\rm ew}$ which are given by

$$\begin{aligned}\mathcal{M}_8 &= 2f_\pi^2 g_8 G g_x \varepsilon_\mu^*(q)\Bigg[p_1^\mu\left(x_A^u + x_A^s + \frac{m_\pi^2}{m_K^2 - m_\pi^2}(x_V^d - x_V^s)\right)\\ &\qquad + p_2^\mu\left(x_A^u + x_A^d + \frac{m_K^2}{m_K^2 - m_\pi^2}(x_V^d - x_V^s)\right)\Bigg], \end{aligned} \tag{3.1}$$

$$\mathcal{M}_8^S = 2f_\pi^2 g_8^S G g_x \varepsilon_\mu^*(q)(p_1+p_2)^\mu (x_A^u + x_A^d + x_A^s), \tag{3.2}$$

$$\begin{aligned}\mathcal{M}_{27} &= \frac{2f_\pi^2 g_{27} G g_x}{3}\,\varepsilon_\mu^*(q)\Bigg[p_1^\mu\left(4x_A^u - 3x_A^d - x_A^s + 2\frac{m_\pi^2}{m_K^2 - m_\pi^2}(x_V^d - x_V^s)\right)\\ &\qquad + p_2^\mu\left(4x_A^u - x_A^d - 3x_A^s + 2\frac{m_K^2}{m_K^2 - m_\pi^2}(x_V^d - x_V^s)\right)\Bigg], \end{aligned} \tag{3.3}$$

$$\mathcal{M}_{\rm ew} = -2f_\pi^2 e^2 g_8 g_{\rm ew} G g_x (p_1+p_2)^\mu \varepsilon_\mu^*(q)\frac{f_\pi^2}{m_K^2 - m_\pi^2}(x_V^s - x_V^d). \tag{3.4}$$

On the other hand, the decay rate can be written as

$$\Gamma = \frac{1}{2m_K}\frac{\left|\overline{\mathcal{M}}\right|^2}{8\pi}\left[1 - 2\left(\frac{m_X^2 + m_\pi^2}{m_K^2}\right) + \left(\frac{m_X^2 - m_\pi^2}{m_K^2}\right)^2\right]^{1/2}, \tag{3.5}$$

where the total unpolarised amplitude squared is given by

$$\begin{aligned}|\overline{\mathcal{M}}|^2 = &\frac{g_x^2}{m_X^2\,(m_K^2-m_\pi^2)^2}[(m_K-m_\pi)^2-m_X^2][(m_K+m_\pi)^2-m_X^2]\Bigg[x_V^{32}(m_K^2-m_\pi^2)\\ &-2g_{\rm ew}e^2 f^4 G g_8(x_V^s-x_V^d)-f^2G\bigg(g_8^S(m_K^2-m_\pi^2)(x_A^u+x_A^d+x_A^s)\\ &+\frac{2}{3}g_{27}m_K^2(x_V^s-x_V^d+2x_A^d+2x_A^s-4x_A^u)+g_8m_\pi^2(x_V^s-x_V^d+x_A^d+x_A^s+2x_A^u)\\ &-\frac{2}{3}g_{27}m_\pi^2(x_V^s-x_V^d-2x_A^d-2x_A^s+4x_A^u)-g_8m_K^2(x_V^s-x_V^d-x_A^d-x_A^s-2x_A^u)\bigg)\Bigg]^2.\end{aligned} \tag{3.6}$$

Assuming generation universality of the couplings, i.e. $x_{V,A}^u = x_{V,A}^d = x_{V,A}^s$, and taking the limit $m_K \gg m_X, m_\pi$, one can find the simple expression

$$\Gamma \approx \frac{m_K}{2\pi}\left(\frac{m_K}{m_X}\right)^2 G_F^2 f_\pi^4 \left|V_{us}\right|^2 g_x^2\,(x_A^u)^2\left(g_8 + \frac{3}{4}g_8^S\right)^2. \tag{3.7}$$

A few important comments are in order:

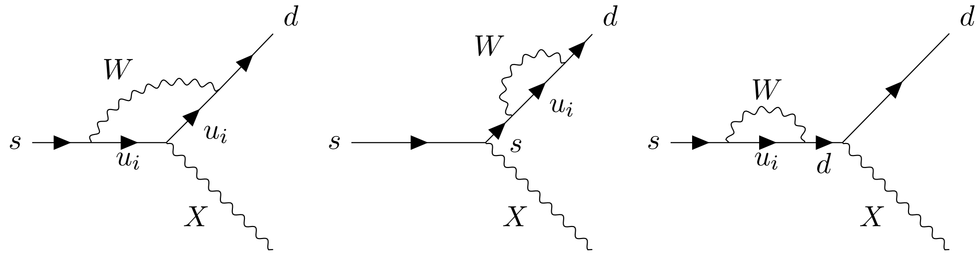

Figure 4. Feynman diagrams contributing to the process $K^\pm \to \pi^\pm X$ at the one-loop level.

- In the limit of universal vector couplings, the decay rate of $K^\pm \to \pi^\pm X$ becomes independent of these couplings as a result of the underlying $SU(3)_V$ chiral symmetry.
- The enhancement factor $(m_K/m_X)^2$ in eq. (3.7) for small m_X is conceptually similar to the enhancement obtained in [28, 29]. This enhancement here is produced by the longitudinal component of the polarization vector: $\sum \varepsilon^*_\mu(q)\varepsilon_\nu(q) = -\eta_{\mu\nu} + \frac{q_\mu q_\nu}{m_X^2}$.

In order to see where we stand, we write the branching ratio of $K^\pm \to \pi^\pm X$ as

$$\mathcal{B}(K^+ \to \pi^+ X) \approx \frac{\Gamma(K^+ \to \pi^+ X)}{\Gamma(K^+ \to \mu^+ \nu)} \times \mathcal{B}(K^+ \to \mu^+ \nu)\,, \tag{3.8}$$

where $\Gamma(K \to \mu\nu) \approx m_K m_\mu^2 |V_{us}|^2 f_K^2 G_F^2/4\pi$ and $\mathcal{B}(K \to \mu\nu) \approx 64\%$. Moreover, we assume the equality $f_K = f_\pi$ which holds in the SU(3) chiral limit. Finally, exploiting the E949 measurement $\mathcal{B}(K^+ \to \pi^+ \nu\nu) = (1.73^{+1.15}_{-1.05}) \times 10^{-10}$ [39], we obtain the 2σ level constraint $\mathrm{BR}(K^+ \to \pi^+ X) \lesssim 4 \times 10^{-10}$. As a result, we find the following bound

$$g_x\, x_A^u \lesssim 3 \times 10^{-6} \left(\frac{m_X}{0.1\,\mathrm{GeV}}\right)\,, \tag{3.9}$$

where the charges x_A^u and x_A^d are typically expected to be of order one. The above result will be fully confirmed by the numerical analysis of Section 4.

3.2 One-loop contribution

In this section, we will calculate the one-loop contributions to the flavour-violating process $K^\pm \to \pi^\pm X$. At the quark level, the Feynman diagrams generating the underlying $s \to d$ transition are displayed in figure 4. Notice that these diagrams are sensitive to different couplings of the X boson to quarks. Summing up all contributions, the full amplitude reads

$$\mathcal{M} = g_x\, x_{sd}^{\mathrm{eff}}\, \epsilon^*_\mu\, \bar{s}\gamma^\mu(1-\gamma_5)d\,, \tag{3.10}$$

where

$$x_{sd}^{\mathrm{eff}} = \frac{g^2}{128\pi^2} V_{id}V_{is}^*\, x_i \left[x_R^{u_i} \left(\frac{2}{\epsilon} + \log\frac{\mu^2}{m_i^2} - \frac{1}{2} - 3\frac{(1 - x_i + \log x_i)}{(x_i-1)^2} \right) + x_L^{u_i} \frac{(-1 + x_i - 4)}{(x_i - 1)} \right.$$
$$\left. + \frac{(x_L^d + x_L^s)}{2} \left(\frac{3 - 3x_i^2 + 2(4x_i - 1)\log x_i}{2(x_i-1)^2} - \frac{2}{\epsilon} - \log\frac{\mu^2}{m_i^2} \right) \right]\,, \tag{3.11}$$

$x_i = m_i^2/m_W^2$ with m_i being the mass of the up-type quark running in the loop and we have defined the chiral charges as $x^f_{L/R} = x^f_V \mp x^f_A$. The divergences, originating from the non-renormalizability of our model, can be interpreted within a hard cutoff regularization scheme as $2/\epsilon + \log(\mu^2/m_i^2) = \log(\Lambda^2/m_i^2)$ where Λ is the UV cutoff. In specific renormalizable models, Λ will be identified with the mass scale of particles belonging to the NP sector which will provide a UV completion of our model.

In the limit of universal couplings, i.e. $x^{u_i}_{V,A} = x^d_{V,A} = x^s_{V,A}$, and keeping only the dominant loop effects stemming from the exchange of the top quark, we obtain

$$x^{\rm eff}_{sd} \simeq \frac{g^2}{64\pi^2} V_{td} V^*_{ts} x^u_A f(x_t) \tag{3.12}$$

where

$$f(x_t) = x_t \left[\frac{2}{\epsilon} + \log\frac{\mu^2}{m_t^2} - \frac{1}{2} - 3\frac{(1 - x_t + \log x_t)}{(x_t - 1)^2}\right] . \tag{3.13}$$

The inclusion of the above loop effects in the decay rate of $K^\pm \to \pi^\pm X$ can be implemented by the following replacement in eq. (3.6):

$$x^{32}_V \to x^{32}_V - x^{\rm eff}_{sd} . \tag{3.14}$$

As a result, we can estimate the relative size of loop effects and tree-level ones as

$$\frac{x^{\rm eff}_{sd}}{4 g_8 f_\pi^2 G x^u_A} \approx f(x_t) , \tag{3.15}$$

where $f(x_t)$ is a model-dependent loop function which depends on the specific UV completion of our effective theory. Therefore, we have learned that loop-effects have a similar size of tree-level contributions. However, while the former suffer from sizeable uncertainties, the latter provide a robust model-independent result. Moreover, we also remark that loop and tree-level contributions generally depend on different couplings and therefore the comparison in eq. (3.15) is valid only in the universal scenario $x^{u_i}_{V,A} = x^d_{V,A} = x^s_{V,A}$.

Although a systematic comparison of tree-level and one-loop results in specific UV realizations of our simplified model would be very interesting, this study deserves a dedicated analysis which is beyond the scope of the present work and it will be presented elsewhere.

4 Flavour bounds vs. beam-dump and collider searches

We are ready now to exploit the results derived in the previous section, in order to explore the capability of the process $K^\pm \to \pi^\pm X$ to unveil new light vector bosons. We are going to use the DarkCast package [21, 22], which enables us to derive bounds on vector and axial couplings of models entailing new spin-1 states by imposing current and future experimental constraints on several processes. In figure 5, we show the bounds in the (m_X, g_x) plane arising from a variety of beam-dump and collider searches [22] as well as from the flavour changing process $K^\pm \to \pi^\pm X$ discussed in this paper. The three plots refer to the benchmark models dubbed as axial, chiral and 2HDM [22] which differ for the values of the $x_{V,A}$ charges, see table 1.

JHEP12(2023)016

	x_V^e	x_V^ν	$x_V^{u,c,t}$	$x_V^{d,s,b}$	x_A^e	x_A^ν	$x_A^{u,c,t}$	$x_A^{d,s,b}$
Axial	0	1/4	0	0	−1	−1/4	1	−1
Chiral	−1	0	1	1	−1	0	1	−1
2HDM	0.044	0.05	1.021	0.015	−0.1	0.05	−0.95	−0.1

Table 1. Charges of the SM fermions under X boson interactions for the models considered in ref. [22] where, for simplicity, flavor universal couplings have been assumed.

The most relevant bounds from beam-dump and collider searches displayed in figure 5 include data from LEP, BaBar, NA64 and NA48/2. The regions bounded by LEP and BaBar are those in pink, with the former covering the region from $10\,\text{GeV} \lesssim m_X \lesssim 100\,\text{GeV}$ [40, 41], while the latter sets the best bounds for $m_X \lesssim 10\,\text{GeV}$ [42]. The experiment NA64 at CERN [43] sets constraints in the MeV-GeV range via searches for invisibly decaying vector bosons. These are radiated by hard bremsstrahlung processes from the reaction $eZ \to eZX$ and correspond to the "e-brem" region in the plots. The regions corresponding to the " μ-brem" area represent instead the future sensitivity reach from the experiment NA64$_\mu$ [44, 45]. This will be analogous to NA64, but will look for vector boson emissions from the process $\mu Z \to \mu Z X$. Bounds from the pion decay $\pi_0 \to X\gamma$ are set by NA48/2 [18]. A more detailed review of the experimental bounds discussed above can be found in [21, 22].

Note that beam-dump and collider constraints are mainly driven by the couplings to electrons. Hence, the less constrained model turns out to be the 2HDM, since it features the weakest couplings to electrons (cf. table 1). As discussed in [22], these benchmarks models highlight different features of vector boson interactions. For instance, the chiral model corresponds to charging only the right-handed fermions, and thus no interactions with neutrinos appear at tree level. On the other hand, the axial model does not have vectorial couplings to quarks and hence the pion decay into a photon and X is forbidden. Other differences stem from the original charge assignment and are due to the relative size of the couplings.

The bounds from the process $K^\pm \to \pi^\pm X$ are obtained by employing the tree-level prediction of Section 3.1 (barring accidental cancellations with the loop-induced contributions of eq. (3.11)) and exploiting the measurement of $\text{BR}(K^+ \to \pi^+ \nu\nu) = (1.73^{+1.15}_{-1.05}) \times 10^{-10}$ by the E949 experiment at BNL [39]. In particular, we impose the 2σ bound $\text{BR}(K^+ \to \pi^+ X) \lesssim 4 \times 10^{-10}$. Remarkably, in all scenarios of figure 5, the process $K^\pm \to \pi^\pm X$ sets the strongest to date model-independent bound in the (m_X, g_x) plane for $m_X < m_K - m_\pi$.

5 Conclusions

Extensions of the SM entailing new feebly interacting massive particles with sub-GeV masses are currently among the most studied scenarios of NP. In particular, comprehensive analyses aiming to probe a light spin-1 boson X featuring general couplings to quarks and leptons have been carried out in the literature exploiting beam-dump and collider searches.

JHEP12(2023)016

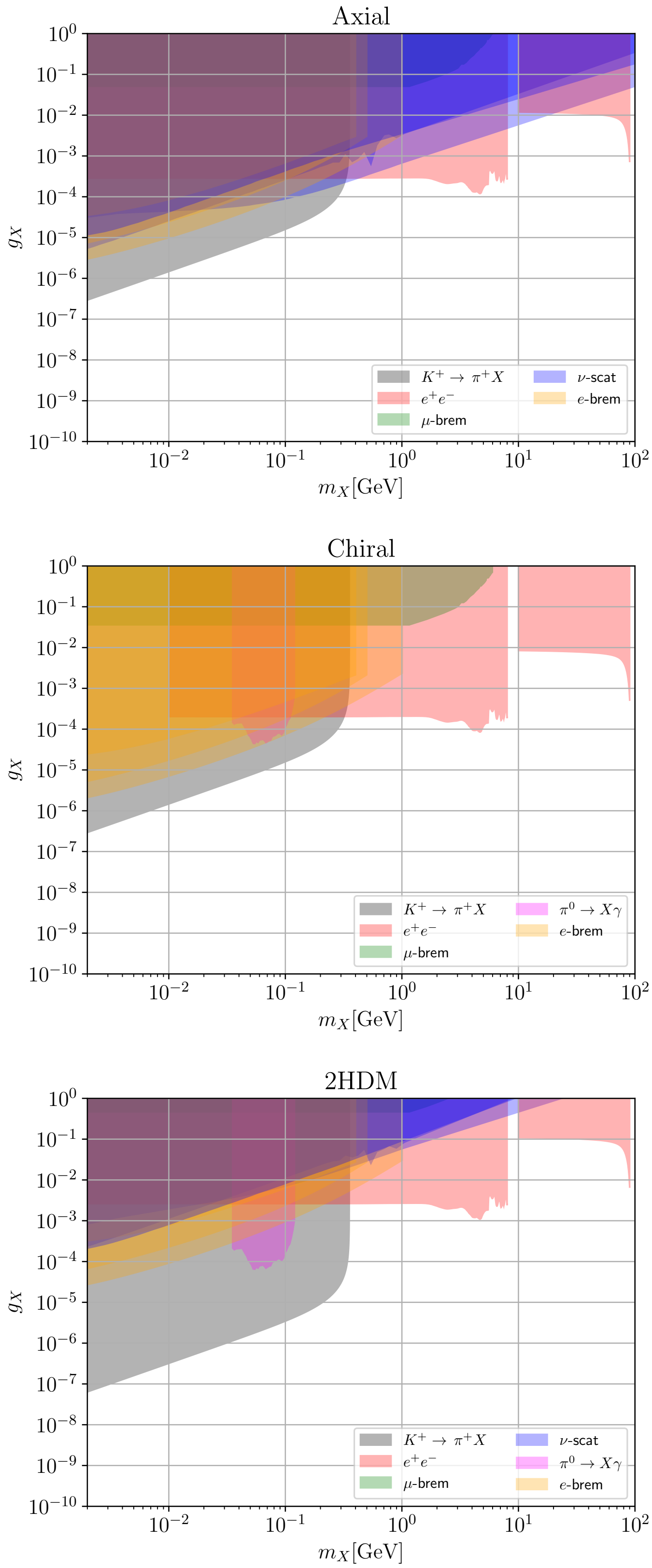

Figure 5. The dark shaded area represents the tree-level $K^\pm \to \pi^\pm X$ bound obtained in this work. Limits from beam-dump and collider searches are obtained with DarkCast [22] and are shown for the purpose of comparison for the three benchmark models given in table 1.

JHEP12(2023)016

In this work, we revisited the flavour constraints to this scenario by means of the rare decay $K^\pm \to \pi^\pm X$. In particular, we extended previous studies by constructing the most general $\Delta S = 1$ chiral Lagrangian as induced by weak interactions up to the order $\mathcal{O}(p^4)$.

The lowest-order $\mathcal{O}(p^2)$ terms of our χPT capture the effects to $K^\pm \to \pi^\pm X$ discussed in [29], which are loop-induced and suppressed by the fifth power of the Cabibbo angle. Instead, the inclusion of subleading $\mathcal{O}(p^4)$ terms in the chiral expansion generates $K^\pm \to \pi^\pm X$ already at the tree-level and the related amplitude is only singly Cabibbo suppressed. As a result, rather surprisingly, the two contributions turn out to be of comparable size, see eq. (3.15).

However, while the tree-level weak effects discussed in this work are model-independent, the loop-induced contributions of ref. [29] are instead sensitive to the specific UV completion accounting for the mass of the spin-1 boson.

In conclusion, we have shown that the process $K^\pm \to \pi^\pm X$ sets the strongest to date model-independent bound on the diagonal axial-vector couplings to u, d, s quarks of a light X with $m_X < m_K - m_\pi$, superseding the bounds arising from beam-dump and collider searches.

Acknowledgments

This work received funding from the European Union's Horizon 2020 research and innovation programme under the Marie Skłodowska-Curie grant agreement N° 860881 and by the INFN Iniziative Specifica APINE. The work of LDL is also funded by the European Union – NextGenerationEU and by the University of Padua under the 2021 STARS Grants@Unipd programme (Acronym and title of the project: CPV-Axion – Discovering the CP-violating axion).

A Details of the chiral Lagrangian construction

In this appendix we will provide an extensive derivation of the chiral Lagrangian describing $\Delta S = 1$ transitions. The operators of eq. (2.10) have the form

$$\mathcal{L}_{\text{eff}}^{\text{EW, LL}} = [t_L]^{jl}_{ik} (\overline{q}^i_L \gamma^\mu q_{Lj})(\overline{q}^k_L \gamma_\mu q_{Ll}) \,, \tag{A.1}$$

and

$$\mathcal{L}_{\text{eff}}^{\text{EW, LR}} = [t^{\delta\delta}_{LR}]^{jl}_{ik} (\overline{q}^i_L \gamma^\mu q_{Lj})(\overline{q}^k_R \gamma_\mu q_{Rl}) + [t^{\lambda\lambda}_{LR}]^{jl}_{ik} (\overline{q}^i_L \gamma^\mu T^a q_{Lj})(\overline{q}^k_R \gamma_\mu T^a q_{Rl}) \,. \tag{A.2}$$

Let us first discuss how to identify those combinations of four-quark operators belonging to irreducible representations of the chiral group [34–36]. From the invariance under the flavour group $\text{U}(3)_F \equiv \text{U}(3)_L \times \text{U}(3)_R$, we know that the LL currents transform as the 81-dimensional representation of $(\overline{3} \otimes 3) \otimes (\overline{3} \otimes 3)$ of $\text{U}(3)_L$ which can be further decomposed into irreducible symmetric or antisymmetric representations having dimension $1, 8, 10, 27$.

In particular, one has symmetric-symmetric combinations $\mathcal{SS}$ transforming in the $1 \oplus 8 \oplus 27$ representations and antisymmetric-antisymmetric combinations $\mathcal{AA}$ transforming as $1 \oplus 8$ representations. We can disregard the symmetric-antisymmetric and antisymmetric-symmetric combinations transforming in the $8 \oplus 10$ representations because they cannot be

JHEP12(2023)016

generated by the operators in (A.1) which are symmetric under the simultaneous exchange of upper indices with the lower ones, $(i,k) \leftrightarrow (j,l)$. In any case, the particular combinations of quark currents transforming in each one of these representations can be obtained by projecting the fundamental structure in (A.1) on the orthonormal basis of irreducible representations of $(\overline{3} \otimes 3) \otimes (\overline{3} \otimes 3)$:

$$\{(e_{27}^a)_{\mathcal{S}}^{\mathcal{S}},\, (e_8^a)_{\mathcal{S}}^{\mathcal{S}},\, (e_1)_{\mathcal{S}}^{\mathcal{S}},\, (e_{10}^a)_{\mathcal{S}}^{\mathcal{A}},\, (e_8^a)_{\mathcal{S}}^{\mathcal{A}},\, (e_{10}^a)_{\mathcal{A}}^{\mathcal{S}},\, (e_8^a)_{\mathcal{A}}^{\mathcal{S}},\, (e_8^a)_{\mathcal{A}}^{\mathcal{A}},\, (e_1)_{\mathcal{A}}^{\mathcal{A}}\}\,. \tag{A.3}$$

This task is accomplished by making use of the tensorial product defined as

$$\mathcal{T}_1 \cdot \mathcal{T}_2 \equiv (T_1)^{ij}_{kl}(T_2)^{kl}_{ij}\,, \qquad \mathcal{T}^{a\,M}_{r\,N} \equiv \mathcal{T} \cdot e^{a\,M}_{r\,N} = T^{ij}_{kl}\,[e^{a\,M}_{r\,N}]^{kl}_{ij}\,, \tag{A.4}$$

where we exploited the decomposition $\mathcal{T} = \mathcal{T}^{a\,M}_{r\,N} e^{a\,M}_{r\,N}$.

Now, the fully symmetric singlet and octet basis elements are

$$[(e_1)^{\mathcal{S}}_{\mathcal{S}}]^{kl}_{ij} = \frac{1}{2\sqrt{6}}[\delta^k_i\delta^l_j + \delta^l_i\delta^l_j]\,, \qquad [(e^a_8)^{\mathcal{S}}_{\mathcal{S}}]^{kl}_{ij} = \frac{1}{2\sqrt{10}}[(\lambda^a)^k_i\delta^l_j + (\lambda^a)^l_i\delta^k_j + (\lambda^a)^k_j\delta^l_i + (\lambda^a)^l_j\delta^k_i]\,, \tag{A.5}$$

whereas the fully antisymmetric singlet and octet basis elements are

$$[(e_1)^{\mathcal{A}}_{\mathcal{A}}]^{kl}_{ij} = \frac{1}{2\sqrt{3}}[\delta^k_i\delta^l_j - \delta^l_i\delta^l_j]\,, \qquad [(e^a_8)^{\mathcal{A}}_{\mathcal{A}}]^{kl}_{ij} = \frac{1}{2\sqrt{2}}[(\lambda^a)^k_i\delta^l_j - (\lambda^a)^l_i\delta^k_j - (\lambda^a)^k_j\delta^l_i + (\lambda^a)^l_j\delta^k_i]\,. \tag{A.6}$$

The symmetric-symmetric 27-plet basis element is harder to construct and a better strategy is to extract the corresponding component by subtracting from a fully symmetric tensor its octet and singlet parts, namely

$$(\mathcal{T}_{27})^{\mathcal{S}}_{\mathcal{S}} = \mathcal{T}^{\mathcal{S}}_{\mathcal{S}} - (\mathcal{T}_8)^{\mathcal{S}}_{\mathcal{S}} - (\mathcal{T}_1)^{\mathcal{S}}_{\mathcal{S}} = \mathcal{T}^{\mathcal{S}}_{\mathcal{S}} - [\mathcal{T}^{\mathcal{S}}_{\mathcal{S}} \cdot (e_1)^{\mathcal{S}}_{\mathcal{S}}]\,(e_1)^{\mathcal{S}}_{\mathcal{S}} - [\mathcal{T}^{\mathcal{S}}_{\mathcal{S}} \cdot (e^a_8)^{\mathcal{S}}_{\mathcal{S}}]\,(e^a_8)^{\mathcal{S}}_{\mathcal{S}}\,. \tag{A.7}$$

The decomposition of the operators appearing in (A.1) can be easily performed by projecting the quark currents onto the orthonormal basis elements. Their chiral counterparts are then simply obtained by projecting the chiral equivalent of quark currents in equation (2.12) onto the very same basis elements.

LL currents: the fully symmetric and anti-symmetric octet Lagrangian reads

$$\begin{aligned}\mathcal{L}_8^{\mathcal{S}(\mathcal{A})} =& a_8^{\mathcal{S}(\mathcal{A})}\frac{f_\pi^4}{80}[t_L]^{jl}_{ik}\left(\mathrm{Tr}\,(\lambda^a L_\mu)\mathrm{Tr}\,L^\mu \pm \mathrm{Tr}\,(\lambda^a L_\mu L^\mu)\right) \cdot \\ & [(\lambda^a)^k_i\delta^l_j \pm (\lambda^a)^l_i\delta^k_j \pm (\lambda^a)^k_j\delta^l_i + (\lambda^a)^l_j\delta^k_i]\end{aligned} \tag{A.8}$$

In principle, one should consider also the structure $\mathrm{Tr}(\lambda^a(U^\dagger\chi + \chi^\dagger U))$ along with $\mathrm{Tr}(\lambda^a L^\mu L_\mu)$. However, these additional structures induce vacuum misalignment effects through Goldstone tadpoles and can be rotated away by properly redefining the Goldstone fields [34].

The 27-plet Lagrangian term is finally given by

$$\begin{aligned}\mathcal{L}_{27} = a_{27}\frac{f_\pi^4}{8}\Big\{[t_L]^{jl}_{ik}\Big(&[(L_\mu)^i_j(L^\mu)^k_l + (L_\mu)^k_j(L^\mu)^i_l] - \frac{1}{12}\left(\mathrm{Tr}\,(L_\mu L^\mu) + \mathrm{Tr}\,L_\mu\mathrm{Tr}\,L^\mu\right)[\delta^i_j\delta^k_l + \delta^i_l\delta^k_j] \\ &- \frac{1}{10}\left(\mathrm{Tr}\,(\lambda^a L_\mu L^\mu) + \mathrm{Tr}\,(\lambda^a L_\mu)\mathrm{Tr}\,L^\mu\right)[(\lambda^a)^k_i\delta^l_j + (\lambda^a)^l_i\delta^k_j + (\lambda^a)^k_j\delta^l_i + (\lambda^a)^l_j\delta^k_i]\Big)\Big\}\,.\end{aligned} \tag{A.9}$$

In the expressions (A.8) and (A.9), the parameters $a_8^{\mathcal{S}}$, $a_8^{\mathcal{A}}$ and a_{27} parametrize our ignorance about the hadronization dynamics and are to be determined experimentally.

LR currents: since left-handed and right-handed currents transform under different U(3) groups, these combinations correspond to the product of a $\overline{3} \oplus 3 = 1 \oplus 8$ representation in each chiral sector, resulting in four possible different structures transforming as $(1_L, 1_R)$, $(8_L, 1_R)$, $(1_L, 8_R)$ and $(8_L, 8_R)$. We first identify the associated orthonormal basis

$$(e_{1_L,1_R})^{kl}_{ij} = \frac{\delta^j_i \delta^l_k}{3}, \quad (e^a_{8_L,1_R})^{kl}_{ij} = \frac{(\lambda^a_L)^j_i \delta^l_k}{\sqrt{6}}, \quad (e^a_{1_L,8_R})^{kl}_{ij} = \frac{\delta^j_i (\lambda^b_R)^l_k}{\sqrt{6}}, \quad (e^{a,b}_{8_L,8_R})^{kl}_{ij} = \frac{(\lambda^a_L)^j_i (\lambda^b_R)^l_k}{2}, \tag{A.10}$$

which will be then used in order to project the appropriate structure onto the low-energy operators possessing definite chiral transformation properties. Exploiting the completeness relation

$$T^a_{ij} T^a_{kl} = \frac{1}{2}\delta_{il}\delta_{kj} - \frac{1}{2N_C}\delta_{ij}\delta_{lk}\,, \tag{A.11}$$

we can recast eq. (A.2) in the following form

$$\mathcal{L}^{\mathrm{EW,\,LR}}_{\mathrm{eff}} = [t^{\delta\delta}_{LR}]^{jl}_{ik} (\overline{q}^i_L \gamma^\mu q_{Lj})(\overline{q}^k_R \gamma_\mu q_{Rl}) - \frac{1}{2N_C} [t^{\lambda\lambda}_{LR}]^{jl}_{ik} (\overline{q}^i_L \gamma^\mu q_{Lj})(\overline{q}^k_R \gamma_\mu q_{Rl})\,. \tag{A.12}$$

At this point the Fierz identity

$$(\overline{q}^i_L \gamma^\mu q_{Lj})(\overline{q}^k_R \gamma_\mu q_{Rl}) = -2(\overline{q}^i_L q_{Rl})(\overline{q}^k_R q_{Lj}) \tag{A.13}$$

can be used in order to identify the various operators.

The leading order chiral structure that is compatible with an $(8_L, 8_R)$ structure reads

$$\mathcal{L}_{8_L,8_R} = \frac{f^6_\pi}{4} (a^{\delta\delta}_{88} [t^{\delta\delta}_{LR}]^{jl}_{ik} + a^{\lambda\lambda}_{88} [t^{\lambda\lambda}_{LR}]^{jl}_{ik}) (\lambda^a_L)^i_j (\lambda^b_R)^k_l \mathrm{Tr}\,(\lambda^a_L U^\dagger \lambda^b_R U) + \mathcal{O}(p^2)\,. \tag{A.14}$$

Instead, the structures transforming as $(8_L, 1_R)$ and $(1_L, 8_R)$ are

$$\mathcal{L}^{LR}_8 = \frac{f^4_\pi}{6} (a^{\delta\delta}_{LR} [t^{\delta\delta}_{LR}]^{jl}_{ik} + a^{\lambda\lambda}_{LR} [t^{\lambda\lambda}_{LR}]^{jl}_{ik}) \{\mathrm{Tr}\,(\lambda_a L_\mu L^\mu)(\lambda^a_L)^i_j \delta^k_l + \mathrm{Tr}\,(\lambda_a R_\mu R^\mu) \delta^i_j (\lambda^b_R)^k_l\}\,. \tag{A.15}$$

Also in this case the constants $a^{\delta\delta}_{88}$, $a^{\lambda\lambda}_{88}$, $a^{\delta\delta}_{LR}$ and $a^{\lambda\lambda}_{LR}$ parametrize our ignorance on the non-perturbative dynamics related to the hadronization process.

Combining all above results, one obtains the $\Delta S = 1$ chiral Lagrangian of eq. (2.14) where the coefficients g_{27}, g_8 and g_{ew} are functions of the non-perturbative effective parameters a_* defined above, as well as of the Wilson coefficients entering eqs. (A.1) and (A.2).

As shown in [35, 36], the matching procedure requires to decompose the operators of eq. (2.9) into operators having well-defined chiral transformation properties under the flavour group

$$\begin{aligned}
Q_1 &= \frac{1}{10} Q^{(8,1),1/2}_S + \frac{1}{15} Q^{(27,1),1/2}_S + \frac{1}{3} Q^{(27,1),3/2}_S + \frac{1}{2} Q^{(8,1),1/2}_A \\
Q_2 &= \frac{1}{10} Q^{(8,1),1/2}_S + \frac{1}{15} Q^{(27,1),1/2}_S + \frac{1}{3} Q^{(27,1),3/2}_S - \frac{1}{2} Q^{(8,1),1/2}_A \\
Q_3 &= \frac{1}{2} Q^{(8,1),1/2}_S + \frac{1}{2} Q^{(8,1),1/2}_A \\
\tilde{Q}_4 &= \frac{1}{2} Q^{(8,1),1/2}_S - \frac{1}{2} Q^{(8,1),1/2}_A
\end{aligned}$$

JHEP12(2023)016

$$Q_9 = -\frac{1}{10}Q_S^{(8,1),1/2} + \frac{1}{10}Q_S^{(27,1),1/2} + \frac{1}{2}Q_S^{(27,1),3/2} + \frac{1}{2}Q_A^{(8,1),1/2}$$
$$\tilde{Q}_{10} = -\frac{1}{10}Q_S^{(8,1),1/2} + \frac{1}{10}Q_S^{(27,1),1/2} + \frac{1}{2}Q_S^{(27,1),3/2} + \frac{1}{2}Q_A^{(8,1),1/2}\,, \tag{A.16}$$

where 1/2 and 3/2 in the superscripts denote the operator isospin properties, while $\tilde{Q}_4$ and $\tilde{Q}_{10}$ are the Fierzed counterparts of Q_4 and Q_{10}:

$$\tilde{Q}_4 = 4\sum_q(\bar{s}_L\gamma^\mu q_L)(\bar{q}_L\gamma_\mu d_L) \quad \text{and} \quad \tilde{Q}_{10} = 6\sum_q e_q(\bar{s}_L\gamma^\mu q_L)(\bar{q}_L\gamma_\mu d_L)\,. \tag{A.17}$$

Defining

$$Q_S^{(27,1)} = \frac{1}{9}\big[Q_S^{(27,1),1/2} + 5\,Q_S^{(27,1),3/2}\big]\,, \tag{A.18}$$

one can then isolate in each operator the desired chiral structures transforming in the irreducible representations of the flavour group [46]. Then, such structures can be directly translated into their χPT counterparts.

As far as the LR operators are concerned, we first need to recast the operators in eq. (2.10) in a form compatible with eq. (A.2). This is achieved by making use of the completeness relation

$$\delta_{\beta\gamma}\delta_{\alpha\delta} = 2T^a_{\alpha\gamma}T^a_{\beta\delta} + \frac{1}{N_C}\delta_{\alpha\gamma}\delta_{\beta\delta}\,, \tag{A.19}$$

which allows us to rewrite

$$\begin{aligned}(\bar{q}^i_\alpha\gamma^\mu\delta_{\beta\gamma}q^j_\gamma)(\bar{q}^k_\beta\gamma_\mu\delta_{\alpha\delta}q^l_\delta) &= 2(\bar{q}^i_\alpha\gamma^\mu T^a_{\alpha\gamma}q^j_\gamma)(\bar{q}^k_\beta\gamma_\mu T^a_{\beta\delta}q^l_\delta) + \frac{1}{N_C}(\bar{q}^i_\alpha\gamma^\mu\delta_{\alpha\gamma}q^j_\gamma)(\bar{q}^k_\beta\gamma_\mu\delta_{\beta\delta}q^l_\delta)\\ &\equiv 2Q^{\lambda\lambda}_{ijkl} + \frac{1}{N_C}Q^{\delta\delta}_{ijkl}\,.\end{aligned} \tag{A.20}$$

The chiral counterparts of the operators on the right-hand side are well known. Then, from

$$C_{5(7)}Q_{5(7)} + C_{6(8)}Q_{6(8)} = \left(C_{5(7)} + \frac{C_{6(8)}}{N_C}\right)Q_{\delta\delta} + 2C_{6(8)}Q_{\lambda\lambda} \tag{A.21}$$

and

$$Q_5 = Q_5^{(8,1)} \qquad \text{and} \qquad Q_7 = \frac{1}{2}Q_S^{(8,8),3/2} + \frac{1}{2}Q_A^{(8,8),1/2}\,, \tag{A.22}$$

we can proceed with the matching procedure obtaining the following results:

$$\begin{aligned}
g_{27} &= \frac{3}{5}a_{27}(\mu)\left(C_1 + C_2 + \frac{3}{2}C_9 + \frac{3}{2}C_{10}\right)(\mu)\\
g_8 &= \frac{1}{10}a_8^{\mathcal{S}}(\mu)(C_1 + C_2 + 5C_3 + 5C_4 - C_9 - C_{10})(\mu) +\\
&\quad - \frac{1}{2}a_8^{\mathcal{A}}(\mu)(C_1 - C_2 + C_3 - C_4 + C_9 - C_{10})(\mu)\\
&\quad + 4\{a_{LR}^{\delta\delta}(\mu)\left(C_5 + \frac{C_6}{N_C}\right)(\mu) + 2a_{LR}^{\lambda\lambda}(\mu)C_6(\mu)\}\\
g_8^S &= \frac{1}{10}a_8^{\mathcal{S}}(\mu)(C_1 + C_2 + 5C_3 + 5C_4 - C_9 - C_{10})(\mu) +\\
&\quad + \frac{1}{2}a_8^{\mathcal{A}}(\mu)(C_1 - C_2 + C_3 - C_4 + C_9 - C_{10})(\mu)\\
e^2 g_8\, g_{\rm ew} &= 6\left\{a_{88}^{\delta\delta}(\mu)\left(C_7 + \frac{C_8}{N_C}\right)(\mu) + 2a_{88}^{\lambda\lambda}(\mu)C_8(\mu)\right\}\,.
\end{aligned}$$

JHEP12(2023)016

References

[1] B. Holdom, *Two* U(1)*'s and Epsilon Charge Shifts*, Phys. Lett. B **166** (1986) 196 [INSPIRE].

[2] M. Pospelov, A. Ritz and M.B. Voloshin, *Secluded WIMP Dark Matter*, Phys. Lett. B **662** (2008) 53 [arXiv:0711.4866] [INSPIRE].

[3] J.D. Bjorken, R. Essig, P. Schuster and N. Toro, *New Fixed-Target Experiments to Search for Dark Gauge Forces*, Phys. Rev. D **80** (2009) 075018 [arXiv:0906.0580] [INSPIRE].

[4] APEX collaboration, *Search for a New Gauge Boson in Electron-Nucleus Fixed-Target Scattering by the APEX Experiment*, Phys. Rev. Lett. **107** (2011) 191804 [arXiv:1108.2750] [INSPIRE].

[5] H. Merkel et al., *Search at the Mainz Microtron for Light Massive Gauge Bosons Relevant for the Muon $g-2$ Anomaly*, Phys. Rev. Lett. **112** (2014) 221802 [arXiv:1404.5502] [INSPIRE].

[6] BaBar collaboration, *Search for Dimuon Decays of a Light Scalar Boson in Radiative Transitions $\Upsilon \to \gamma A^0$*, Phys. Rev. Lett. **103** (2009) 081803 [arXiv:0905.4539] [INSPIRE].

[7] D. Curtin et al., *Exotic decays of the* 125 *GeV Higgs boson*, Phys. Rev. D **90** (2014) 075004 [arXiv:1312.4992] [INSPIRE].

[8] BaBar collaboration, *Search for a Dark Photon in e^+e^- Collisions at BaBar*, Phys. Rev. Lett. **113** (2014) 201801 [arXiv:1406.2980] [INSPIRE].

[9] LHCb collaboration, *Search for Dark Photons Produced in* 13 *TeV pp Collisions*, Phys. Rev. Lett. **120** (2018) 061801 [arXiv:1710.02867] [INSPIRE].

[10] A. Anastasi et al., *Limit on the production of a low-mass vector boson in $e^+e^- \to U\gamma$, $U \to e^+e^-$ with the KLOE experiment*, Phys. Lett. B **750** (2015) 633 [arXiv:1509.00740] [INSPIRE].

[11] LHCb collaboration, *Search for $A' \to \mu^+\mu^-$ Decays*, Phys. Rev. Lett. **124** (2020) 041801 [arXiv:1910.06926] [INSPIRE].

[12] CMS collaboration, *Search for a Narrow Resonance Lighter than* 200 *GeV Decaying to a Pair of Muons in Proton-Proton Collisions at $\sqrt{s} = 13$ TeV*, Phys. Rev. Lett. **124** (2020) 131802 [arXiv:1912.04776] [INSPIRE].

[13] G. Bernardi et al., *Search for Neutrino Decay*, Phys. Lett. B **166** (1986) 479 [INSPIRE].

[14] KLOE-2 collaboration, *Search for a vector gauge boson in ϕ meson decays with the KLOE detector*, Phys. Lett. B **706** (2012) 251 [arXiv:1110.0411] [INSPIRE].

[15] KLOE-2 collaboration, *Limit on the production of a light vector gauge boson in phi meson decays with the KLOE detector*, Phys. Lett. B **720** (2013) 111 [arXiv:1210.3927] [INSPIRE].

[16] WASA-at-COSY collaboration, *Search for a dark photon in the $\pi^0 \to e^+e^-\gamma$ decay*, Phys. Lett. B **726** (2013) 187 [arXiv:1304.0671] [INSPIRE].

[17] HADES collaboration, *Searching a Dark Photon with HADES*, Phys. Lett. B **731** (2014) 265 [arXiv:1311.0216] [INSPIRE].

[18] NA48/2 collaboration, *Search for the dark photon in π^0 decays*, *Phys. Lett. B* **746** (2015) 178 [arXiv:1504.00607] [INSPIRE].

[19] NA62 collaboration, *Search for production of an invisible dark photon in π^0 decays*, *JHEP* **05** (2019) 182 [arXiv:1903.08767] [INSPIRE].

[20] Y. Kahn, G. Krnjaic, S. Mishra-Sharma and T.M.P. Tait, *Light Weakly Coupled Axial Forces: Models, Constraints, and Projections*, *JHEP* **05** (2017) 002 [arXiv:1609.09072] [INSPIRE].

[21] P. Ilten, Y. Soreq, M. Williams and W. Xue, *Serendipity in dark photon searches*, *JHEP* **06** (2018) 004 [arXiv:1801.04847] [INSPIRE].

[22] C. Baruch, P. Ilten, Y. Soreq and M. Williams, *Axial vectors in DarkCast*, *JHEP* **11** (2022) 124 [arXiv:2206.08563] [INSPIRE].

[23] K. Asai et al., *Chiral Z' in FASER, FASER2, DUNE, and ILC beam dump experiments*, *Phys. Rev. D* **106** (2022) 095033 [arXiv:2206.12676] [INSPIRE].

[24] P. Fayet, *Effects of the Spin 1 Partner of the Goldstino (Gravitino) on Neutral Current Phenomenology*, *Phys. Lett. B* **95** (1980) 285 [INSPIRE].

[25] P. Fayet, *Parity Violation Effects Induced by a New Gauge Boson*, *Phys. Lett. B* **96** (1980) 83 [INSPIRE].

[26] P. Fayet, *U-boson production in e^+e^- annihilations, psi and Upsilon decays, and Light Dark Matter*, *Phys. Rev. D* **75** (2007) 115017 [hep-ph/0702176] [INSPIRE].

[27] P. Fayet, *On the Search for a New Spin 1 Boson*, *Nucl. Phys. B* **187** (1981) 184 [INSPIRE].

[28] J.A. Dror, R. Lasenby and M. Pospelov, *New constraints on light vectors coupled to anomalous currents*, *Phys. Rev. Lett.* **119** (2017) 141803 [arXiv:1705.06726] [INSPIRE].

[29] J.A. Dror, R. Lasenby and M. Pospelov, *Dark forces coupled to nonconserved currents*, *Phys. Rev. D* **96** (2017) 075036 [arXiv:1707.01503] [INSPIRE].

[30] G. Buchalla, A.J. Buras and M.E. Lautenbacher, *Weak decays beyond leading logarithms*, *Rev. Mod. Phys.* **68** (1996) 1125 [hep-ph/9512380] [INSPIRE].

[31] L. Di Luzio, M. Nardecchia and C. Toni, *Light vectors coupled to anomalous currents with harmless Wess-Zumino terms*, *Phys. Rev. D* **105** (2022) 115042 [arXiv:2204.05945] [INSPIRE].

[32] J. Gasser and H. Leutwyler, *Chiral Perturbation Theory: Expansions in the Mass of the Strange Quark*, *Nucl. Phys. B* **250** (1985) 465 [INSPIRE].

[33] A. Pich, *Chiral perturbation theory*, *Rept. Prog. Phys.* **58** (1995) 563 [hep-ph/9502366] [INSPIRE].

[34] A. Pich and A. Rodríguez-Sánchez, SU(3) *analysis of four-quark operators: $K \to \pi\pi$ and vacuum matrix elements*, *JHEP* **06** (2021) 005 [arXiv:2102.09308] [INSPIRE].

[35] RBC collaboration, *Kaon matrix elements and CP violation from quenched lattice QCD: I. The three flavor case*, *Phys. Rev. D* **68** (2003) 114506 [hep-lat/0110075] [INSPIRE].

[36] C. Lehner and C. Sturm, *Matching factors for $\Delta S = 1$ four-quark operators in RI/SMOM schemes*, *Phys. Rev. D* **84** (2011) 014001 [arXiv:1104.4948] [INSPIRE].

[37] J.-M. Gerard, C. Smith and S. Trine, *Radiative kaon decays and the penguin contribution to the $\Delta I = 1/2$ rule*, *Nucl. Phys. B* **730** (2005) 1 [hep-ph/0508189] [INSPIRE].

JHEP12(2023)016

[38] G. Ecker et al., *Electromagnetism in nonleptonic weak interactions*, *Nucl. Phys. B* **591** (2000) 419 [hep-ph/0006172] [INSPIRE].

[39] E949 collaboration, *New measurement of the $K^+ \to \pi^+\nu\bar{\nu}$ branching ratio*, *Phys. Rev. Lett.* **101** (2008) 191802 [arXiv:0808.2459] [INSPIRE].

[40] DELPHI collaboration, *Photon events with missing energy in e^+e^- collisions at $\sqrt{s} = 130-$GeV to 209-GeV*, *Eur. Phys. J. C* **38** (2005) 395 [hep-ex/0406019] [INSPIRE].

[41] DELPHI collaboration, *Search for one large extra dimension with the DELPHI detector at LEP*, *Eur. Phys. J. C* **60** (2009) 17 [arXiv:0901.4486] [INSPIRE].

[42] BaBar collaboration, *Search for Invisible Decays of a Dark Photon Produced in e^+e^- Collisions at BaBar*, *Phys. Rev. Lett.* **119** (2017) 131804 [arXiv:1702.03327] [INSPIRE].

[43] NA64 collaboration, *Search for invisible decays of sub-GeV dark photons in missing-energy events at the CERN SPS*, *Phys. Rev. Lett.* **118** (2017) 011802 [arXiv:1610.02988] [INSPIRE].

[44] S.N. Gninenko, D.V. Kirpichnikov, M.M. Kirsanov and N.V. Krasnikov, *Combined search for light dark matter with electron and muon beams at NA64*, *Phys. Lett. B* **796** (2019) 117 [arXiv:1903.07899] [INSPIRE].

[45] H. Sieber et al., *Prospects in the search for a new light Z' boson with the NA64μ experiment at the CERN SPS*, *Phys. Rev. D* **105** (2022) 052006 [arXiv:2110.15111] [INSPIRE].

[46] J. Kambor, J.H. Missimer and D. Wyler, *The Chiral Loop Expansion of the Nonleptonic Weak Interactions of Mesons*, *Nucl. Phys. B* **346** (1990) 17 [INSPIRE].

JHEP12(2023)016